Solar Physics (2004) 224: 247–253

RECONSTRUCTION OF MAGNETIC ACTIVITY OF THE SUN AND CHANGES IN ITS IRRADIANCE ON A MILLENNIUM TIMESCALE USING NEUROCOMPUTING

A. V. MORDVINOV[1], N. G. MAKARENKO[2], M. G. OGURTSOV[3] and H. JUNGNER[4]
[1]*Institute of Solar-Terrestrial Physics, P.O. Box 4026, Irkutsk, 664033, Russia*
(e-mail: avm@iszf.irk.ru)
[2]*Institute of Mathematics, Almaty, Kazakhstan*
[3]*Physico-Technical Institute, Saint-Petersburg, Russia*
[4]*University of Helsinki, Gustav Hällströminkatu 2, POB 64, Finland*

(Received 20 August 2004; accepted 30 September 2004)

Abstract. Relations between basic indices of the Sun and the cosmogenic isotope ^{14}C and ^{10}Be records were derived using the Artificial Neural Network (ANN) technique. A reconstruction of the sunspot indices and changes in Total Solar Irradiance (TSI) was carried out. Long-term changes in TSI appear in the amplitude modulation of its 11-year cyclic variation as well as in its lower envelope describing variability of the background irradiance of the Sun. According to the reconstruction the irradiance has increased about 2.5 W m^{-2} since 1441.

1. Introduction

Continuous monitoring of the Sun by satellite experiments, complemented by earlier observations and cosmogenic isotope data, has clearly shown that the basic physical characteristics of the Sun are time dependent. Total Solar Irradiance (TSI) has been monitored since 1978 (Fröhlich and Lean, 1998; Willson and Mordvinov, 2003; Dewitte *et al.*, 2004). Temporal changes in TSI are mostly caused by the surface magnetism of the Sun (Solanki and Fligge, 1999; Fröhlich and Lean, 2002). Models for reconstruction of magnetic activity of the Sun and changes in its irradiance have been constructed on the basis of both direct and proxy data using different approaches as well as heuristic assumptions (Lean, Beer, and Bradley, 1995; Bard *et al.*, 2000; Usoskin *et al.*, 2004). However, the study of physical relations in a complicated system 'Sun–heliosphere–Earth' that modulates the cosmic ray flux is difficult due to the uncertainties of its evolution.

2. Relation between TSI and Sunspot Indices

The relations between magnetic and thermodynamic indices of the Sun differ on different timescales. Short-term dips in TSI occur when sunspot groups pass across the solar disc, however, the TSI level is maximal when sunspot activity peaks. To identify a model for TSI reconstruction we study the Cross-Correlation Function

(CCF) between the relative sunspot numbers Rz and TSI. Figure 1 displays the total CCF between daily Rz and TSI time series (bold) that has its minimum at zero lag and maximum at lag $= -28$ d.

To study the correlations on 2–32 d, 64–512 d and >1024 d timescales we apply a wavelet decomposition (Daubechies, 1992) for Rz and TSI time series and estimate partial CCFs between the corresponding components (Figure 1). The correlation of short-term components at zero lag displays a minimum that corresponds to sunspot blocking. Long-term components from both decompositions correlate well indicating that surface magnetism is the main cause of changes in TSI on a decadal timescale. The intermediate-term component is highly asymmetric and peaks at lag $= -43$ d. High magnetic activity increases the level of chromospheric radiation with the time delay. The contribution of the facular component in TSI is determined by magnetic activity for previous months. Thus, to model TSI at one point in time we have to take into account sunspot index values for the previous several months.

3. TSI Reconstruction Using the Group Sunspot Numbers

The Artificial Neural Network (ANN) technique is an effective tool to model the behaviour of multi-scale systems with a complicated interrelation between their components. This is also adequate to model cyclic behaviour and long-term evolution of the Sun (Conway, 1998). We apply the ANN technique to estimate the relation between the sunspot indices and TSI and reconstruct solar indices in the past.

To establish a non-linear relation between the magnetic and thermodynamic indices we construct an ANN with sunspot index R being the input and TSI being the output. Taking into account the time delays in causal relation between

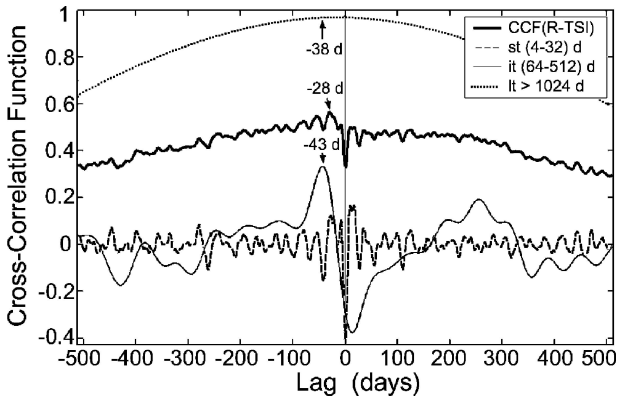

Figure 1. The total and partial CCFs between relative sunspot numbers and TSI.

sunspot index and TSI, write a formal model $TSI(i) = F(R(i-6), R(i-5), \ldots, R(i), D35(i), D67(i), A(i), E(i))$, where $TSI(i)$, $R(i)$ – are monthly averaged TSI and the group sunspot numbers *Rg* (Hoyt and Schatten, 1998) with index i referring to the current month number and $D35(i)$, $D67(i)$ – the components of wavelet decomposition of *Rg* record describing details on 8–32 and 64–128 month timescales, its long-term approximation $A(i)$ and the upper envelope $E(i)$. This model is able to account for both regular and chaotic behaviour of solar activity.

The optimal architecture of an ANN, that minimizes the error of the TSI model has been determined from numerical experiments. The weight coefficients are determined through its training to approximate TSI changes as the output of the ANN. The Multi-Layer Perceptron (MLP) (Conway, 1998) performs a good TSI approximation. The network consists of three layers with eleven inputs, four units in the hidden layer, and one output MLP(11-4-1). Applying the ANN for the sunspot index time series, we reconstruct TSI for the whole epoch of telescopic observations of the Sun.

The result of TSI modeling and reconstruction is shown in Figure 2. The cyclic TSI changes are caused by the magnetic modulation in 11-year cycles. There is also another kind of TSI variation appearing as slow TSI changes between activity minima. These long-term TSI changes appear in the lower envelope and resulted from the quiet-Sun variations (Lean, Beer, and Bradley, 1995). The lower level of TSI has increased during the past century. Thus, our TSI reconstruction confirms the existence of secular changes in solar luminosity although smaller in rate by comparison with direct measurements (Willson and Mordvinov, 2003; Dewitte *et al.*, 2004). However, these are questioned by Fröhlich and Lean (2002).

4. Reconstruction of Solar Activity Based on the ^{14}C Record

The radiocarbon ^{14}C record (Stuiver and Braziunas, 1993) was corrected for the effect of industrial carbon input (Suess effect) using the one-reservoir carbon

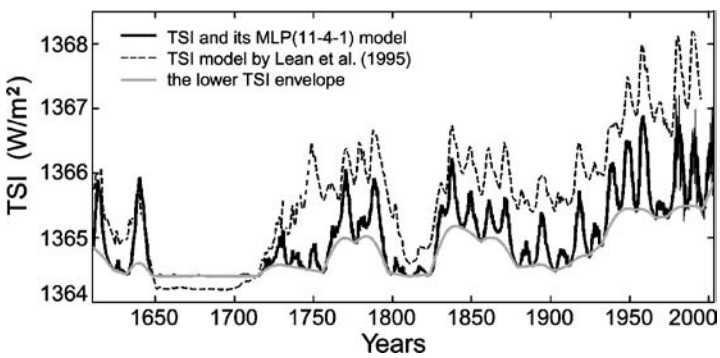

Figure 2. The TSI reconstruction from *Rg* record.

exchange model (Budyko and Israel, 1987). The rate of anthropogenic carbon emission was estimated from analysis of world consumption of gas, coal and oil (Keeling, 1973; Joos, 2003). Parameters of the carbon-exchange model were determined by fitting the mean radiocarbon level at AD 1890–1954 to that calculated by Beer *et al*. (1994) from the beryllium data.

To relate the TSI measurements with the cosmogenic isotopes data we extrapolated the radiocarbon ^{14}C record (Stuiver and Braziunas, 1993) corrected for the Suess effect using the ANN technique. To model both regular and chaotic activity behaviour we can write formally $C(i) = F(R(i-10), R(i-9), \ldots, R(i), D34(i), \ldots, A(i), M(i))$, where the output $C(i)$ is current annual value of ^{14}C with the inputs being sunspot numbers $R(i-10), R(i-9), \ldots, R(i)$, its cyclic component $D34$ on 8–16 year timescale, as well as the longer details and approximation. As the magnetic field of the Earth influences the accumulation of cosmogenic isotopes it should be also included as input of the ANN. The geomagnetic field intensity normalized to its current value $M(i)$ is estimated from compilation of paleomagnetic measurements (Burlatzkaya, 1970).

For 1610–1899 we construct, train and verify the ANN model to approximate changes in ^{14}C using the sunspot index and changes in the Earth's magnetic field. We constructed the optimal MLP(18-2-1) model that minimizes the errors in ^{14}C approximation.

The ^{14}C corrected for the Suess effect, its model and extrapolation during the modern epoch are shown in Figure 3(a). Figure 3(b) illustrates paleomagnetic measurements and the regression plot. The optimal model is chosen from a compromise between training, testing and verifying errors to avoid over-learning of the ANN (Conway, 1998). The extrapolation of ^{14}C reasonably indicates a high-activity level in the 20th century with the most powerful cycle 19.

With this extension in hand we constructed the ANNs to derive non-linear relations between basic solar parameters and the ^{14}C data. The optimal ANN to reconstruct sunspot index *Rg* has an architecture of MLP(16-1-1). Figure 3(c) shows the reconstruction of *Rg* time series. We constructed also the ANN to derive a non-linear relation between the extended ^{14}C time series with annual TSI time series both observed and reconstructed for 1610–2003. Then we can reconstruct TSI since 1511 using the obtained model. The result of TSI reconstruction with MLP(15-11-1) is plotted in Figure 3(d).

5. Reconstructions of Magnetic Activity and Changes in Luminosity of the Sun Using the ^{10}Be Record

Going back in time, we use the cosmogenic isotope ^{10}Be record (Bard *et al*., 1997) to reconstruct magnetic activity and changes in solar luminosity. By analogy with the analysis in the previous section we apply the ANN to extrapolate the ^{10}Be record for 1900–2003 using the ANN that derives a causal relation between sunspot index

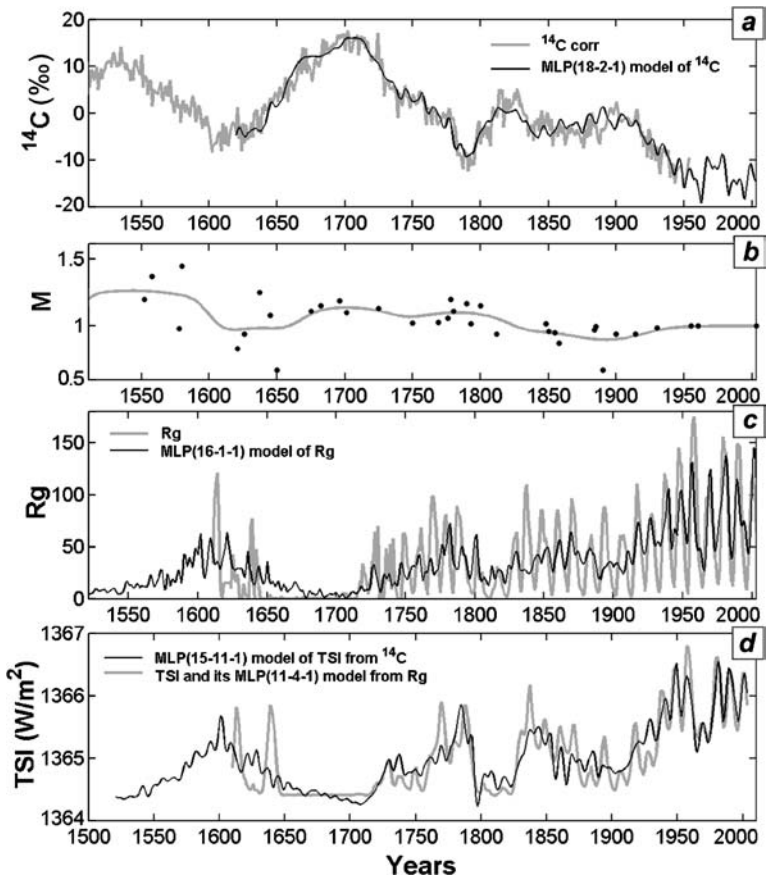

Figure 3. The ^{14}C record, its model and extension (a), the Earth's magnetic field (b); *Rg* and its reconstruction from ^{14}C (c); TSI reconstruction from ^{14}C (d).

Rg and ^{10}Be taking into account changes in the Earth's magnetic field. Figure 4(a) shows the ^{10}Be signal, its model and extrapolation. Paleomagnetic measurements are shown in Figure 4(b).

Special regression ANN models were constructed and trained to approximate changes in TSI and *Rg* for 1610–2003. In Figure 4(c,d) the TSI and *Rg* reconstructions from ^{10}Be record are shown. Solar luminosity reconstructed from ^{10}Be data describes 11-year cycles during the last century. At the earlier period it characterizes a mean level of TSI indicating some cyclic details. The deepest TSI drop to 1364 W m^{-2} occurred during the Spörer activity minimum in 1441. The TSI level decreased also during the Dalton, Maunder, Wolf, and Oort activity minima. Previous reconstructions (Lean, Beer, and Bradley, 1995; Solanki and Fligge, 1999; Bard *et al.*, 2000) show similar temporal patterns but differ in their amplitude.

The cyclic TSI variation is superimposed on secular changes. Since 1441 the lower envelope of solar luminosity has increased by the amount of 2 W m^{-2}.

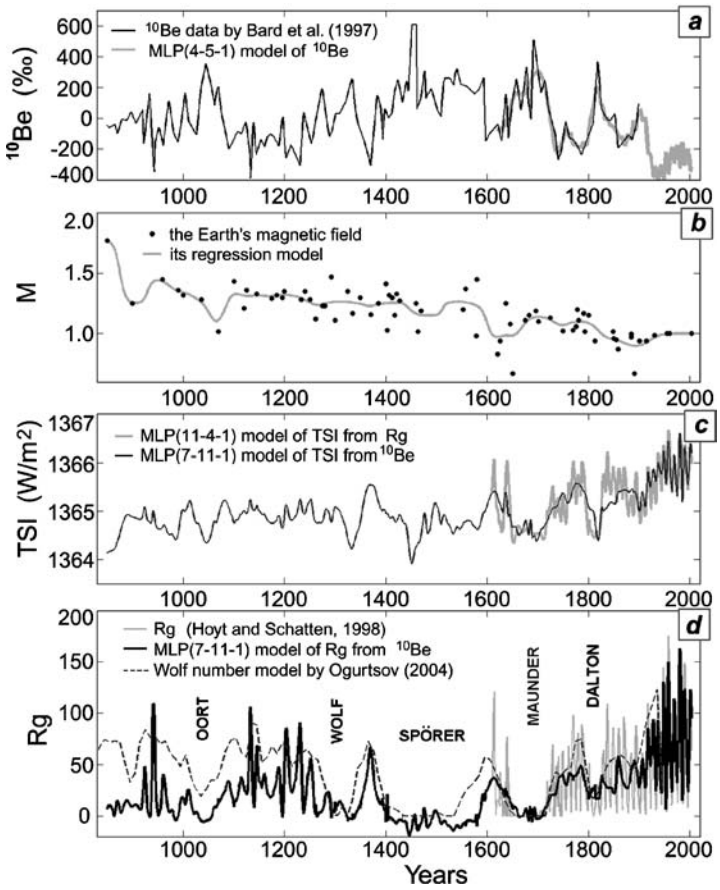

Figure 4. The ^{10}Be and its model (a), the Earth's magnetic field (b); the reconstructions of TSI and *Rg* from the ^{10}Be record (c,d).

Reconstruction of the group sunspot number obtained from the ^{10}Be record agrees also with recent reconstructions (Usoskin *et al.*, 2004; Ogurtsov, 2004). They indicate great minima in the activity of the Sun. The highest maximum in the ^{10}Be record leads to unreal negative values in the *Rg* reconstruction. It is not proportional to the corresponding decrease in TSI due to the non-linear relation between the input-output variables and does not exceed much the error in *Rg* approximation.

6. Conclusion

Reconstructions of luminosity of the Sun from cosmogenic isotope records demonstrate long-term changes in TSI. Long-term changes in magnetic activity of the Sun modulate its 11-year cyclic component. Slowly varying background radiation of

the Sun appears in the lower envelope of TSI. The luminosity has increased about 2.5 W m^{-2} since 1441. The mean rate of TSI increase is about of 0.044 W m^{-2} per decade.

Acknowledgements

Authors are grateful to the ACRIM and VIRGO teams for the TSI data from the ACRIMSAT/ACRIM-3 and ESA/NASA SOHO missions. We thank Prof. E. Bard, Prof. J. Beer, Prof. M. Stuiver and their colleagues for making it possible to study the cosmogenic isotope records. We also thank Prof. S.K. Solanki and Prof. I.G. Usoskin for discussion of this work. This research was supported by INTAS 2001-0550, RFBR 02-02-16044 and the Federal program 'Astronomy' 1105.

References

Bard, E., Raisbeck, G. M., Yiou, F., and Jouzel, J.: 1997, *J. Earth Planetary Sci. Lett.* **150**, 453.

Bard, E., Raisbeck, G. M., Yiou, F., and Jouzel, J.: 2000, *Tellus* **52B**, 985.

Beer, J., Joos, F., Lukasczyk, Ch., Mende, W., Rodriguez, J., Siegenthaler, U., Stellmacher, R.: 1994, in E. Nesme-Ribes, (ed.), *The Solar Engine and Its Influence on Terrestrial Atmosphere and Climate*, NATO ASI Series, **25**, Springer, pp. 221–233.

Budyko, M. I. and Israel, Yu. A.: 1987, *Anthropogenic changes of climate*. Leningrad, Hydrometeoizdat (in Russian).

Burlatzkaya, S. P.: 1970, *Geomagn. Aeron.* **4**(10), 694.

Conway, A. J.: 1998, *New Astronomy Reviews* **42**, 343.

Daubechies, I.: 1992, *Ten Lectures on Wavelets*, Society for industrial and applied mathematics, Philadelphia.

Dewitte, S., Crommelynck, D., Mekaoui, S., and Joukoff, A.: 2004, *Solar Phys.*, this issue.

Fröhlich, C. and Lean, J.: 1998, *Geophys. Res. Lett.* **25**, 4377.

Fröhlich, C. and Lean, J.: 2002, *Astron. Nachr.* **6**, 1.

Hoyt, D. V. and Schatten, K. H.: 1998, *Solar Phys.* **179**, 189.

Joos, F.: 2003, in S.K. Bhattacharya, T.K. Mal, S. Chakrabarti, (eds.) *Recent research developments in biotechnology and bioengineering*, pp. 1–21.

Keeling, C. D.: 1973, *Tellus* **25**(2), 174.

Lean, J., Beer, J., and Bradley, R.: 1995, *Geophys. Res. Lett.* **22**, 3195.

Ogurtsov, M. G.: 2004, *Solar Phys.* **220**, 93.

Solanki, S. K. and Fligge, M.: 1999, *Geophys. Res. Lett.* **26**, 2465.

Stuiver, M. and Braziunas, T. F.: 1993, *Holocene* **3**(4), 289.

Usoskin, I. G., Mursula, K., Solanki, S., Schüssler, M., and Alanko, K.: 2004, *Astron. Astrophys.* **413**, 745.

Willson, R. C. and Mordvinov, A. V.: 2003, *Geophys. Res. Lett.* **30**, 1199.